

# BEAM PROFILE MEASUREMENT USING HELIUM GAS LIGHT EMISSION AND BEPM FOR SUPERHEAVY ELEMENT SEARCH EXPERIMENT

T. Watanabe\*, T. Adachi, P. Brionnet, O. Kamigaito,  
K. Morimoto, T. Nishi, A. Uchiyama, RIKEN, Wako, Japan  
A. Kamoshida, National Instruments Japan Corporation, Tokyo, Japan  
K. Kaneko, R. Koyama, SHI Accelerator Service Ltd., Wako, Japan

## Abstract

The newly constructed superconducting linear accelerator (SRILAC) is now in operation with the aim of discovering new superheavy elements and advancing the production of medical radiation isotopes. Because it is crucial to extend the durability of the expensive Cm target for as long as possible, these experiments require the accelerated V beam to be sufficiently widened. To this end, a helium gas light emission monitor (HeLM) has been introduced to measure the beam profile. Because He gas flows within the target chamber, by capturing the light emitted from He gas with a CCD camera, the beam profile can be obtained nondestructively and continuously. These measurements are handled through programming in LabVIEW, with analyzed data integrated into an EPICS control system. A method to estimate the beam envelope has been recently developed by leveraging the measured quadrupole moments with beam energy position monitors (BEPMs), and incorporating calculations of the transfer matrix. The synergistic use of HeLM and BEPM plays a useful role in accurately controlling the beam size at the Cm target.

## INTRODUCTION

To upgrade the RIKEN Heavy-ion Linac (RILAC), the Superconducting RILAC (SRILAC) has been constructed, and successful commissioning has been completed [1]. These accelerators are being operated to advance research into even heavier synthetic elements [2]; build on the discovery of element 113, Nihonium [3]; and enhance the production capability of the short-lived radioisotope <sup>211</sup>At, which is anticipated to have applications in cancer therapy [4]. Over the past three years, the V beam, accelerated by both the RILAC and SRILAC, has been irradiated onto the Cm target for superheavy elements research.

## BEAM PROFILE MEASUREMENT USING He GAS LIGHT EMISSION

### RILAC, SRILAC, and GARIS III

A schematic drawing of the RILAC, SRILAC, GARIS III, and production apparatus for medical RIs is shown in Fig. 1. The V beam, accelerated by both RILAC and SRILAC, is irradiated onto the Cm targets inside a target chamber. To

prevent the Cm targets from melting due to the beam irradiation, several thin Cm targets are mounted on a 30-cm radius wheel, which rotates at 2000 rpm. GARIS III separates the superheavy elements from the unwanted particles, achieving high background noise reduction, by using dipole and quadrupole magnets. Furthermore, helium gas is introduced so that the electron charges of the superheavy elements converge to a certain value. Even if superheavy elements with different charges are ejected from the target, because the charges of superheavy elements become equal while they are passing through the helium gas, it is possible to collect the desired superheavy elements.

### Target Chamber and HeLM for GARIS III

To protect the Cm target, it is essential to extend its durability for as long as possible. Therefore, the accelerated V beam must not only hit the Cm target but also be adequately widened. A schematic drawing of the beam line with a differential pumping system and the target chamber for GARIS III is shown in Fig. 2. Baffle electrodes are installed at the top, bottom, left, and right to detect the edge of the beam, and a carbon slit is installed in front of the target to cut the edge of the beam. CCD cameras monitor how the beam irradiates the target through view ports located upstream and downstream of the target. In Fig. 2, the beam comes from the left side, hits the Cm targets, and then proceeds to GARIS III. Since He gas flows within the target chamber,

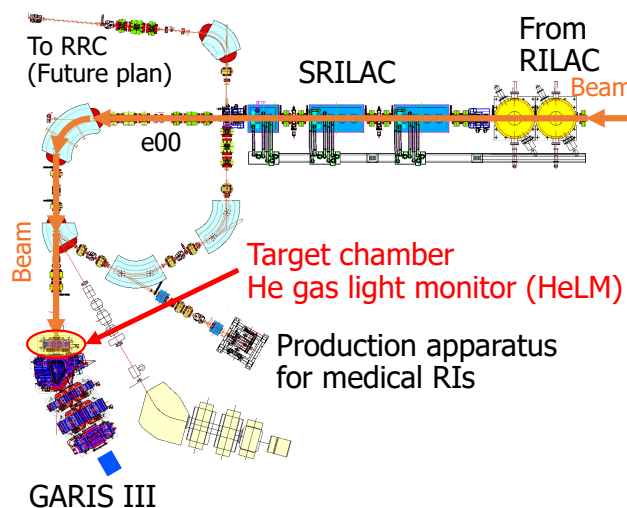


Figure 1: Schematic drawing of the RILAC, SRILAC, GARIS III, and production apparatus for medical RIs.

\* wtamaki@riken.jp

Content from this work may be used under the terms of the CC-BY-4.0 licence (© 2023). Any distribution of this work must maintain attribution to the author(s), title of the work, publisher, and DOI

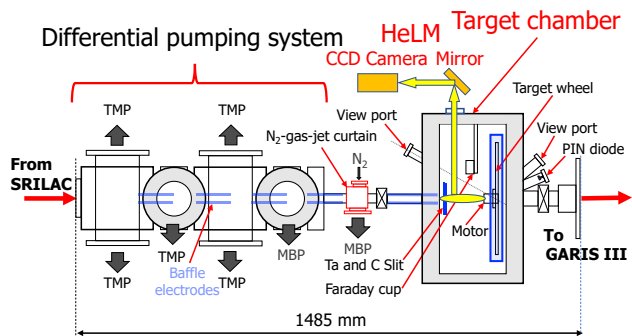


Figure 2: Schematic drawing of the beam line with the differential pumping system and target chamber for GARIS III.

its electrons are excited through collisions with the beam, and the light is emitted when the electrons return to their ground state during the de-excitation process. By capturing the emitted light with a CCD camera, the beam profile can be obtained nondestructively and continuously.

A picture of the target chamber and the He gas light monitor is shown in Fig. 3. Hereafter, the He gas light monitor is referred to as “HeLM”. To detect the light emitted from helium gas, a light window is located at the top of the target chamber. Since the target chamber is in an extremely high radiation environment, the light-receiving elements for the CCD camera gradually deteriorate as the experiment progresses. The CCD camera used for the HeLM is a small commercial monitor camera that employs CMOS elements. To minimize deterioration, the emitted light is reflected by a mirror located near the light window, and the reflected light is received by the CCD camera, which is set far from the target. However, even with this system, radiation damage cannot be completely avoided, and the CCD camera needs to be replaced approximately every two months. The detachable lens is reused after the CCD camera is replaced. The image signal obtained with the CCD camera is sent to a video server through an analog cable, and the digitized image data are transmitted to a HeLM controller via Ethernet. The specifications of the lens, CCD camera and video server are provided in Table 1.

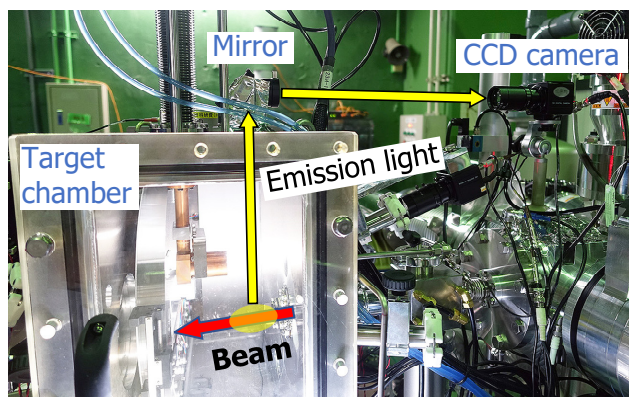


Figure 3: Photograph of the target chamber and HeLM. The emitted light is reflected by a mirror located near the light window and the reflected light is received by the CCD camera.

Table 1: Specifications of the Lens, CCD Camera, and Video Server

CCTV* Lens	Lens for CCD camera For 1/3 or 1/4 inch sensor
Focus	Focal length 6-60 mm (variable)
Iris	Manual F1.6
Sensor	CCD camera Sony307 1/3 inch CMOS
Video resolution	Pal/NTSC 1920 × 1080
Electrical shutter	1/50 ~ 1/10,000 s
Model No.	Video server AXIS Q7404
Chanel number	4
Video compression	H.264 MPEG-4 Part 10/AVC Motion JPEG
Resolution	720 × 480 ~ 176 × 120
Frame rate	30 frames/s
Processor	ARTPEC-3 × 4
Memory	Main 128MB × 4, Flash 128MB × 4
CCTV*	Closed Circuit Television

### Programming for Image Acquisition and Analysis with LabVIEW and Web API

To analyze the beam profile, the HeLM controller obtains image data from the video server using a Web API (Application Programming Interface). The program to access the video server and save the acquired data is implemented with the Web API and the C++ OpenCV library. To achieve near real-time performance, one image frame is acquired every 200 ms.

The image data acquisition and analysis program is built using LabVIEW. LabVIEW includes a “Vision Development Module” designed for developing image processing applications to automate visual inspection tasks in industrial and other fields. This module contains “NI Vision Assistant” software, which allows developers to create application software interactively, confirming the results step by step. After confirming that the application software was working correctly, it was converted to a VI (Virtual Instrument) and integrated into the main HeLM program. The program could be completed in a short period of time using the NI Vision Assistant.

The front panels of the aforementioned application software and the analyzed results of the emitted He gas light are shown in Fig. 4. Since the details of the target are confidential, the length is expressed in pixel dimensions. The upper and lower front panels can be switched using a tab selection button. In the upper front panel, the measured results and setting selections are displayed as follows: (a) The result of integrating the brightness in the direction of travel of the beam and the result of a Gaussian fit, (b) An image of He gas emission, (c) The value of a Gaussian fit  $1\sigma$  and the deviation from the center, and (d) The setting panel for the

fitting region, which can be selected manually or through direct numerical input.

The result of the integrated luminance along the beam direction represents the transverse beam profile, and the Gaussian fitted  $1\sigma$  is defined as the beam width. In the lower panel, the history of the Gaussian fitted  $1\sigma$  is recorded at the following scales: 1 minute (top), 1 hour (middle), and 1 day (bottom), as shown in Fig. 4(e). If the experimental user sets the maximum and minimum thresholds for the beam width  $1\sigma$ , and the beam width exceeds those thresholds, the HeLM controller can automatically send a warning email to the user.

At the RI Beam Factory (RIBF) at the Nishina Center for Accelerator-Based Science, the distributed control en-

vironment system known as EPICS (Experimental Physics and Industrial Control System) has been implemented to operate and manage accelerators and large-scale experimental apparatuses. EPICS facilitates communication between servers and clients using the communication protocol known as Channel Access (CA). Here, the Input Output Controller (IOC) is a pivotal software component within EPICS that connects the controlled devices to the CA communication network and offers so-called Process Variable (PV) data. The analyzed data obtained by the HeLM monitor are stored in the PVs. However, due to security considerations, the HeLM controller is linked to the general LAN, which is isolated from the dedicated EPICS LAN. Consequently, data from both networks are relayed through a proxy server using the HTTP client method.

## MEASURED BEAM WIDTH WITH HeLM AND BEAM OPTICS CALCULATIONS USING BEPM

We discuss the HeLM measurements and beam optics calculations by using an example of accelerator operations conducted on 29 June 2022. In the early morning of that day, the experimental user requested that the beam optics be readjusted because the beam width measured using HeLM had decreased from 37 pixels (before the adjustment) to 31 pixels. While we attempted to adequately widen the beam on the target, the beam loss needed to be minimized as much as possible. To this end, we calculated the beam optics and adjusted them using the calculated results. Figure 5 shows the elastic scattering measurement results (red line), the beam width measured by the HeLM (blue line), and the carbon slit current (green line). After the beam optics were adjusted from 10:34 to 11:00, the beam width was improved from 31 to 37 pixels, as shown by the blue line in Fig. 5. The beam transmission efficiency, defined as the ratio of the up-

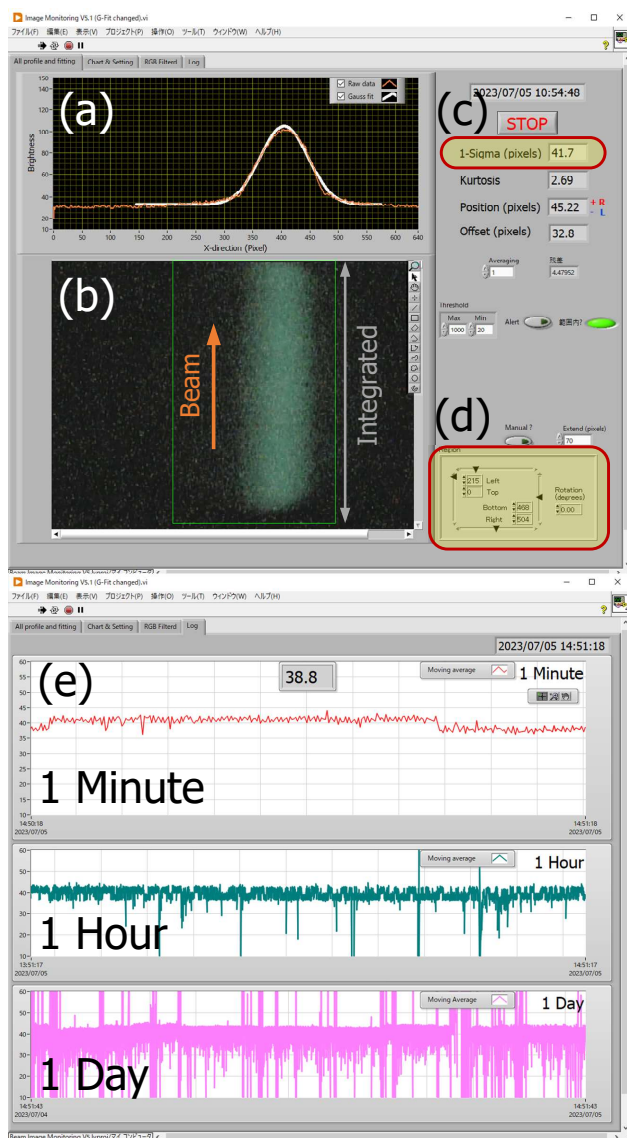


Figure 4: The front panels programmed with LabVIEW. (a) Result of integrating the brightness in the direction of travel of the beam and the result of a Gaussian fit, (b) Image of He gas emission, (c) Value of a Gaussian fit  $1\sigma$  and the deviation from the center, (d) Setting panel for the fitting region, and (e) Record of the Gaussian fit  $1\sigma$ .

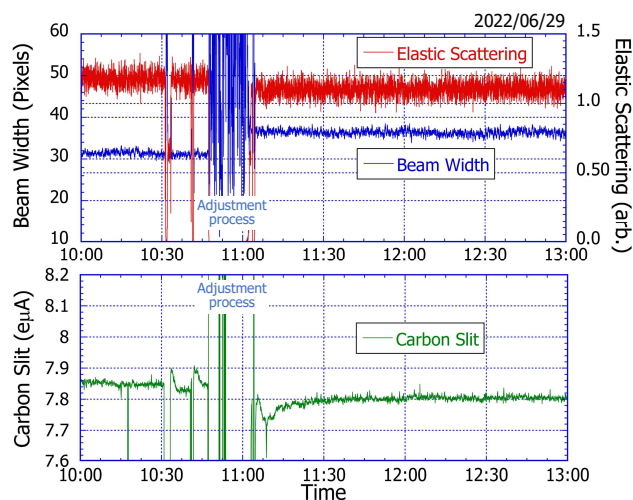


Figure 5: Measured results of elastic scattering (red line), beam width measured by the HeLM (blue line), and carbon slit current (green line).

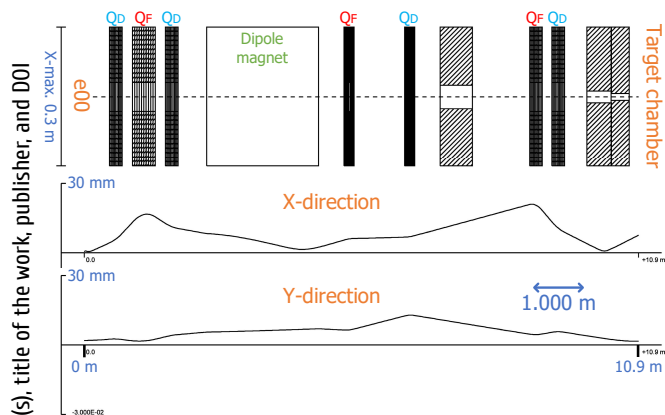


Figure 6: Calculated result of the beam envelope from e00 to the target chamber.

stream beam current to the target one, decreased from 97% to 94%. As shown in Fig. 5, the elastic scattering (red line) and the current of the carbon slit installed just in front of the target (green line) also obviously decreased. The beam current from the carbon slit has a characteristic in which the current increases rapidly just after beam irradiation and then gradually decreases. Therefore, the HeLM, carbon slit current, and elastic scattering measurements are in qualitative agreement.

The calculated results of the beam optics from e00 (see Fig. 1) to the target magnet [5] are shown in Fig. 6. Here, the emittance and Twiss parameters are obtained by the Q-scan method by using a wire scanner installed upstream of SRILAC, and the transfer matrix is calculated from these values to provide optimum conditions at the target. The beam is focused just before the target to increase the spot width, and the beam width measured by the HeLM is fine-tuned to optimize the quadrupole magnet.

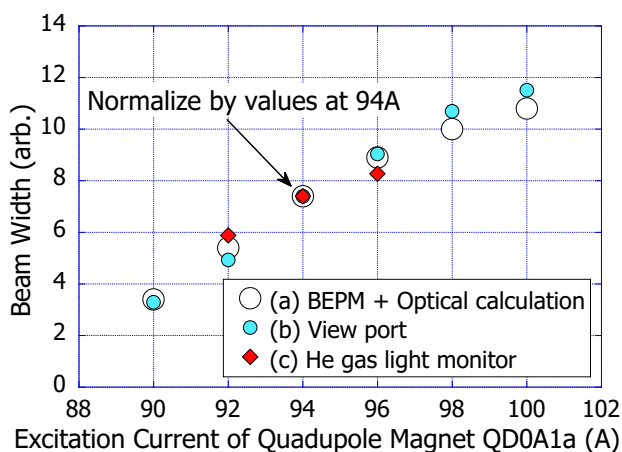


Figure 7: The beam widths obtained by: (a) the beam optical calculation using the quadrupole moments measured by the BEPMs, (b) the target spot on the fluorescent target observed through the view port, and (c) the measurement result taken with the HeLM.

Furthermore, we examined the beam width measurements and the beam optics calculation using the BEPMs [6] by changing the excitation current of the quadrupole magnet located in front of the target chamber. Figure 7 shows the beam widths obtained by (a) the beam optical calculation using the quadrupole moments measured by the BEPMs, (b) the target spot on the fluorescent target observed through the view port, and (c) the measurement result taken with the HeLM. Since these beam widths have different scales, they are all normalized to the excitation current of 94 A. The beam widths analyzed by these methods are in good agreement.

## CONCLUSION

In the superheavy element search experiment, the beam profile is obtained with a CCD camera by observing the light emitted when the beam passes through the helium gas in the target chamber. This method has the advantage that the beam profile can be obtained nondestructively and continuously. These measurements are handled through programming in LabVIEW and the analyzed data are integrated into an EPICS control system. Furthermore, a method to estimate the beam envelope has been recently developed by leveraging the measured quadrupole moments with BEPMs, and incorporating calculations of the transfer matrix. The synergistic use of HeLM and BEPM allows us to accurately control the beam size at the Cm target.

## ACKNOWLEDGEMENTS

The authors would like to thank Dr. Hiromitsu Haba and Dr. Daiya Kaji for providing detailed information on the superheavy element search experiment, and Dr. Yutaka Watanabe for supplying the CAD data.

## REFERENCES

- [1] K. Yamada *et al.*, “Successful Beam Commissioning of Heavy-Ion Superconducting Linac at RIKEN”, in *Proc. SRF’21*, East Lansing, MI, USA, Jun.-Jul. 2021, pp. 167. doi:10.18429/JACoW-SRF2021-M00FAV01
- [2] H. Sakai *et al.*, “Facility upgrade for superheavy-element research at RIKEN”, *Eur. Phys. J. A*, vol. 58, 2022, pp. 1–15. doi:10.1140/epja/s10050-022-00888-3
- [3] K. Morita *et al.*, “New Result in the Production and Decay of an Isotope, <sup>278</sup>113, of the 113th Element”, *J. Phys. Soc. Jpn.*, vol. 81, p. 103201, 2012. doi:10.1143/JPSJ.81.103201
- [4] H. Haba *et al.*, “Present status of <sup>211</sup>At production at the RIKEN AVF cyclotron”, *RIKEN Accel. Prog. Rep.*, vol. 53, 2019, p. 192. <https://www.nishina.riken.jp/researcher/APR/APR053/pdf/192.pdf>
- [5] T. Nishi *et al.*, “Emittance Measurement and Ion Optics Tuning for SRILAC Beamline”, in *Proc. of the 17th Annual Meeting of Particle Accelerator Society of Japan*, Sept. 2020, pp. 116–119. [https://www.pasj.jp/web\\_publish/pasj2020/proceedings/PDF/TH00/TH0008.pdf](https://www.pasj.jp/web_publish/pasj2020/proceedings/PDF/TH00/TH0008.pdf)
- [6] T. Watanabe *et al.*, “Commissioning of the Beam Energy Position Monitor System for the Superconducting RIKEN Heavy-ion Linac”, in *Proc. IBIC’20*, Santos, Brazil, Sep. 2020, pp. 295–302. doi:10.18429/JACoW-IBIC2020-FRA004